

Article

Synthesis of Bismuth Film Assembly on Flexible Carbon Cloth for the Electrochemical Detection of Heavy Metal Ions

Yujie Cao ¹, Xiangyu Zhou ¹, Ziling Wang ¹, Yi Li ¹, Minglei Yan ¹, Yun Zeng ¹, Jie Xiao ², Yang Zhao ^{1,*}  and Jun-Heng Fu ^{1,*}

¹ College of Water Conservancy and Hydropower Engineering, Sichuan Agricultural University, Ya'an 625014, China

² Ecological Environment Monitoring Center Station, Ya'an 625014, China

* Correspondence: yangzhao@sicau.edu.cn (Y.Z.); fujunheng@sicau.edu.cn (J.-H.F.)

Abstract: The utilization of bismuth as a sensing material for the detection of heavy metal ions has gained significant attention due to its exceptional interfacial activity and selective absorption properties. However, it also poses challenges in terms of agglomeration and its inferior electrical conductivity during the synthesis process. This paper employed a facile in situ synthesis and electrodeposition approach to uniformly grow a bismuth film on a conductive carbon cloth, designated as Bi/Ag@CC. The Bi/Ag@CC electrode material exhibited benign electrochemical properties, enabling its application for detecting Pb²⁺ in tap water and lake water samples. Furthermore, this work investigated the impact of electrochemical parameters, including electrolyte pH, deposition potential and pre-enrichment time, on the detection performance. The results demonstrated the sensor's wide linear range (from 20 to 400 ppb) and detection limits (0.15 ppb) for heavy metal ion detection, along with excellent anti-interference capabilities and satisfactory repeatability, with an RSD of less than 2.31% (n = 6). This paper offers a novel strategy for positioning the bismuth-based composite as a promising candidate for practical electrochemical sensing applications.

Keywords: electrochemical sensor; bismuth film; lead ions; carbon cloth; heavy metal ions



Citation: Cao, Y.; Zhou, X.; Wang, Z.; Li, Y.; Yan, M.; Zeng, Y.; Xiao, J.; Zhao, Y.; Fu, J.-H. Synthesis of Bismuth Film Assembly on Flexible Carbon Cloth for the Electrochemical Detection of Heavy Metal Ions. *Chemosensors* **2024**, *12*, 103. <https://doi.org/10.3390/chemosensors12060103>

Received: 7 May 2024

Revised: 4 June 2024

Accepted: 4 June 2024

Published: 6 June 2024



Copyright: © 2024 by the authors. Licensee MDPI, Basel, Switzerland. This article is an open access article distributed under the terms and conditions of the Creative Commons Attribution (CC BY) license (<https://creativecommons.org/licenses/by/4.0/>).

1. Introduction

The issue of global ecological pollution has garnered considerable attention, as water resources are intricately tied to the survival of both humans and other living organisms [1–3]. Nevertheless, due to industrialization, heavy metal pollution in aquatic environments not only causes ecological devastation but also poses a significant threat to human habitats, potentially resulting in public health crises [4]. Among these heavy metal ions, Pb²⁺ emerges as a particularly toxic ion capable of inflicting substantial harm to the heart, brain, and other organs in living organisms when present in concentrated forms [5]. Nevertheless, ensuring environmental safety and mitigating the biological harm caused by the accumulation and non-degradability of heavy metal ions remains a daunting task for the global community.

Traditional heavy metal detection strategies, such as inductively coupled plasma mass spectrometry (ICP-MS), high-performance liquid chromatography (HPLC) and atomic absorption spectrometry (AAS), are widely recognized and employed extensively due to the benefits of extensive linearity, remarkable sensitivity and low detection limits. However, these sensing technologies demand substantial operational expertise and a considerable testing time [6,7]. In recent years, fluorescence and colorimetric methods have emerged as cutting-edge technologies for visually detecting heavy metal ions with specific targeted sites. However, one of the primary problems lies in the limited detecting range of targeted heavy metals [8–11]. Alternatively, the electrochemical sensor addresses this challenge by depositing the targeted ions on the electrode surface and inducing an electrochemical reaction of dissolution in the electrolyte under an applied potential. This reaction generates a distinct

peak redox current, enabling the precise detection of the target substance [3,12,13]. Owing to its convenience, cost efficiency and remarkable precision, this detection strategy has garnered significant attention in the field of heavy metal detection [14]. Furthermore, electroanalytical techniques offer adequate sensitivity, miniaturized and portable equipment and satisfactory accuracy and precise performance [15,16]. By employing conventional techniques such as spin coating and droplet-dripping, it is feasible to achieve the desired modifications on the electrode surface. Viviana et al. [17] proposed a synthetic approach for constructing carbon nanodots derived from biomass-based carbon materials. The modified electrode exhibited high stability and adsorption properties, enabling the electrochemical detection of heavy metal ions such as lead and cadmium ions. The conventional electrode modification method results in the degradation of the optimal performance of the working electrode due to interfacial adhesion [18]. Taking into account the robust, sensitive and selective characteristics of metal–organic frameworks (MOFs) for the targeted metal ions, a rapid electrochemical detection of diverse heavy metal ions has been reported using the MOFs as electrode materials [19,20]. Nevertheless, MOF materials on the surface of the glass carbon electrode over time compromise detection performances.

To address these limitations, in situ growth on the electrode surface was carried out and directly applied to detect heavy metal lead ions without interfacial adhesion. Wang and colleagues constructed a flexible nickel-doped WO_3/CC (carbon cloth) electrode for glucose detection based on in situ synthesis, and the hierarchical microsheets of WO_3 exhibited a substantial specific surface area, greatly enhancing the rate of electron transfer [21]. Gao et al. [6] presented a cupric ion-sensing electrode, featuring the in situ growth of porous rod-like tungsten oxide assembled onto stainless steel mesh, which demonstrated impressive detection capabilities and promising practical applications. Shao et al. [22] illustrated a molybdenum oxide adsorbent with mixed valence, exhibiting selectivity for silver detection and recovery in wastewater. Therefore, the process of in situ synthesis can significantly enhance the stability and reproducibility for the electrochemical detection of heavy metal ions.

Metallic nanomaterials, thanks to their minute size, extensive specific surface area, and exceptional electrical conductivity, could significantly enhance the sensitivity and linearity of electrochemical detection. Bismuth nanoparticles, among various metal particles such as gold and silver nanoparticles, exhibit superior cost effectiveness, environmental friendliness and resistance to oxygen, as well as low toxicity, positioning them as a promising candidate for the electrochemical detection of highly toxic mercury [3]. With the assistance of the electrochemical plating method, Jiang et al. designed and fabricated an integrated and wearable detecting platform by printing bismuth films, and this platform was successfully utilized for the real-time detection of heavy metal ions [23]. Feng et al. [24] successfully achieved remarkable stability and sensitivity in measuring trace amounts of lead ions by employing nitrogen-doped carbon nanosheets encapsulating bismuth nanoparticles (Bi@NC). The porous carbon composite, co-doped with Bi/ Bi_2O_3 , was derived from a bismuth-based organic framework, offering a wide linear range for the electrochemical detection of lead ions. Notably, the sensor exhibited exceptional stability, reproducibility and satisfactory selectivity [25].

In this work, an electrochemical sensor based on Bi/Ag@CC electrode material was constructed and applied to the detection of Pb^{2+} in tap water and lake water samples. The introduction of Ag nanoparticles significantly enhanced the conductivity of the sensor, which was achieved through a simple solution-based synthesis method. Additionally, a Bi layer was deposited on the surface of Ag@CC using an electrochemical deposition approach. The integration of Bi with Ag improved both the electrochemical activity and acid resistance of the sensor. Furthermore, the carbon film serving as a support skeleton not only ensured high electrical conductivity and rapid electrochemical kinetics but also effectively mitigated volume changes during the detection of heavy metal ions [26]. Finally, the Bi/Ag@CC composite was employed as an electrochemical detecting electrode material for

Pb²⁺ sensing using the DPV mode, demonstrating excellent electrochemical performance and electrocatalytic behavior towards heavy metal ions.

2. Materials and Methods

2.1. Materials

All chemicals used to measure heavy metal ions were of analytical grade. Silver nitrate (AgNO₃), ascorbic acid, lead nitrate (Pb[NO₃]₂), bismuth nitrate (Bi[NO₃]₃), potassium ferricyanide (K₃Fe[CN]₆), potassium chloride (KCl) and standard solutions of 1 mg/mL Pb in 2% nitric acid were obtained from Aladdin Chemical Reagent Co., Ltd. (Shanghai, China). The carbon cloth was purchased from Keshenghe (W0S1011, Shenzhen, China). Deionized water was prepared by our own lab equipped with a Flom ultrapure water system (18 MΩ·cm). All the chemicals were utilized directly without further purification.

2.2. Preparation

Carbon cloth as a substrate was firstly soaked and cleaned with acid solution, ethyl alcohol and deionized water, respectively. After drying, the carbon cloth was cut into the size of 20 mm × 10 mm × 1 mm. The carbon cloth was soaked in 0.1 mM AgNO₃ for 20 min and then dried. Next, the dried carbon cloth was added into the 0.2 mM ascorbic acid solution for 10 min, leading to the reduction of Ag nanoparticles, which was named Ag@CC. The Bi/Ag@CC electrode was synthesized via an electrochemical deposition process. The deposition potential and time were selected to be −0.9 V and 480 s, respectively, and the concentration of Bi(NO₃)₃ was 0.2 g/L. Then, the dried samples were named Bi/Ag@CC electrodes. For the Bi@CC electrode materials, the preparation process remains identical to the aforementioned procedure, with the exception of the absence of the in situ reduction of silver nitrate solution.

2.3. Morphological Characteristics

The scanning electron microscopy (ZEISS, GeminiSEM 300, Jena, Germany) with an accelerating voltage of 3 kV was applied to observe the morphology of the prepared electrodes and EDS elemental mapping images. And, the crystal structure of samples was recorded by an X-ray diffractometer (XRD, Tongda, Hong Kong, China) with a scanning speed of 5° min^{−1}. X-ray photoelectron spectroscopy (XPS, PHI QUANTERA-II SXM, Waltham, MA, USA) was used to analyze the elements and valence states of the catalysts. The electronic conductivity was measured by a digital multimeter (RIGIOL, Beijing, China).

2.4. Electrochemical Characteristics

The electrochemical performances were measured via the electrochemical workstation (CHI-760E, CHI Instruments, Shanghai, China) with a conventional three-electrode system. The counter electrode, reference electrode and the working electrode were the graphite rod, Ag/AgCl electrode and the prepared electrodes, respectively. To mitigate the impact of extraneous ions on the accuracy of measurement results, the electrolyte solution employed in this study is a standardized lead nitrate solution. And, the pH of the electrolyte was adjusted by the acidic and basic solutions. Differential pulse voltammetry (DPV) was used by scanning from −1.0 V to −0.2 V, and the pulse height was set as 50 mV. The pulse amplitude and pulse time were set by the instrument without change. And, the scanning rate was adjusted during the experimental measurements. The deposition voltage and time were −1.2 V and 360 s for the preconcentration of heavy metal ions, respectively. The cyclic voltammetry (CV) with a measurement range of −0.6 V~0.6 V and the electrochemical impedance spectroscopy (EIS) at the frequency range of 0.01 Hz to 100 kHz were tested. All the tests were conducted at room temperature.

3. Results and Discussion

3.1. Morphological and Structural Characteristics

Scheme 1 demonstrated the synthesis of Bi/Ag@CC electrode materials via a combination of solution immersion and electrochemical deposition reactions. Firstly, the pristine carbon cloth was immersed in an acidic solution to remove the impurity and soaked into the AgNO_3 solution to yield silver nanoparticles on the carbon cloth surface, which was named Ag@CC. Subsequently, a Bi film was formed by employing electrodeposition on top of the Ag@CC to synthesize Bi/Ag@CC electrode material. Figure 1a depicts the SEM images of the untreated carbon cloth, which exhibit a dense fiber structure with an overall smooth appearance. The SEM images of Ag@CC are presented in Figure 1b, revealing silver nanoparticles attached to the surface of the fibers. Due to the specificity of nucleation sites, the silver particles exhibit a non-uniform distribution across the fiber surface. Ascorbic acid functions as a reducing agent, efficiently converting silver ions into silver monomers [27]. Figure 1c,d depicts the SEM images of the fibers following bismuth electrodeposition. The bismuth film completely covered the fiber surfaces, providing an ample contact area for the subsequent adsorption of heavy metal ions. Additionally, Figure S1 illustrates the effect of varying silver plating concentrations on conductivity. The concentration of silver plating on the carbon cloth surface was adjusted by varying the soaking time in silver nitrate solution, and the soaking duration of 10 min yielded the most significant reduction in resistance on the CC surface, leading to an enhancement in the conductivity of the electrode. Therefore, the immersion duration for Ag@CC in the solution was standardized at 10 min for all subsequent experiments. To deposit a Bi film, an electrodeposition potential of -0.9 V and a pre-enrichment time of 480 s were selected, as depicted in Figure S2.

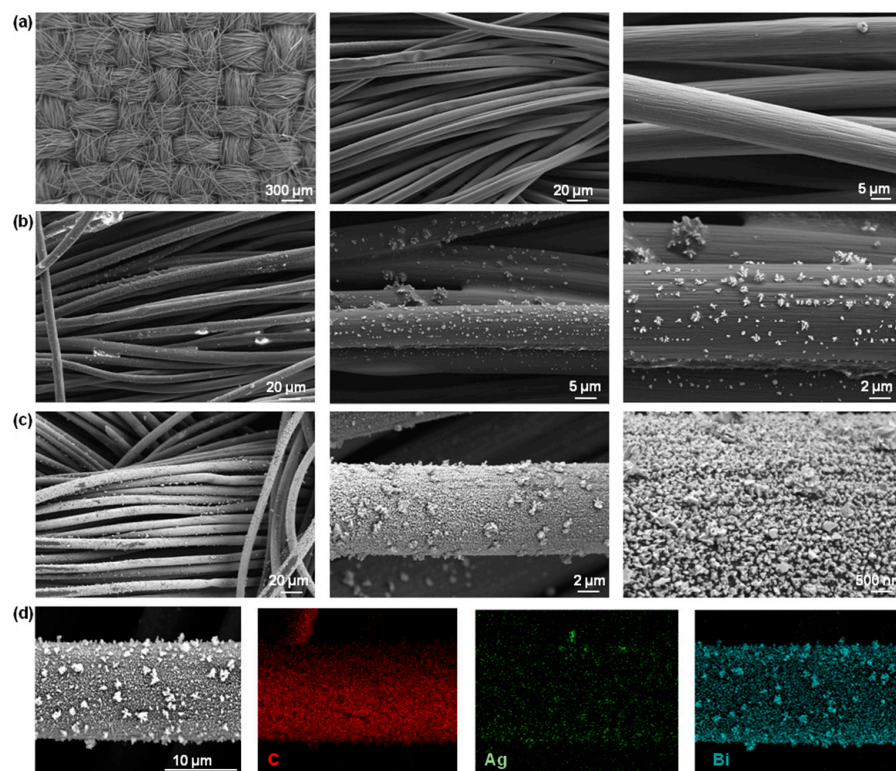
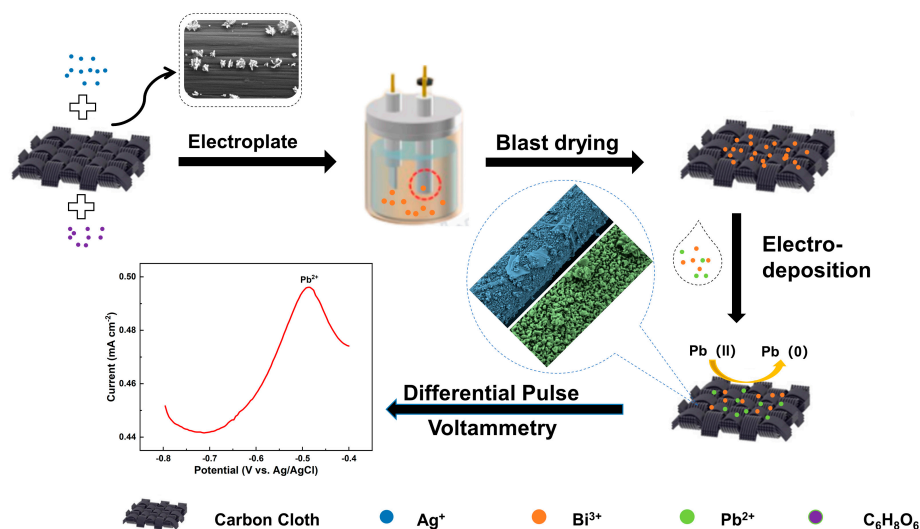


Figure 1. SEM images of (a) CC, (b) Ag@CC and (c) Bi/Ag@CC. (d) The elemental mapping of Bi/Ag@CC.



Scheme 1. Schematic illustration of the synthesis of Bi/Ag@CC. The red dotted circle illustrated the Bi³⁺.

The crystallographic structures of the prepared samples were determined through XRD analysis, with the diffraction peaks of Bi/Ag@CC, Ag@CC and CC presented in Figure 2a. All samples exhibited broad and weak diffraction peaks at $2\theta = 25.5^\circ$ and 43.4° , corresponding to the (002) and (001) planes of graphite (PDF#41-1487) [28]. Specifically, the XRD spectra of Bi/Ag@CC exhibited two primary peaks at 27.2° and 39.7° , aligned with the crystal facets of bismuth (012) and (110), respectively. And, the absence of other impurity peaks suggested the exclusive deposition of metal Bi on the CC substrate [29,30]. The additional analysis of Bi@CC in Figure S3 reveals the absence of the diffraction peaks of Bi, indicating that the bismuth film cannot be effectively deposited on the carbon cloth surface without the silver nanoparticle pre-treatment. These findings suggested that silver nanoparticles on the carbon cloth not only enhance the electronic conductivity of the electrode materials but also facilitate the strong adhesion of bismuth film. Furthermore, the elemental composition and chemical states of the prepared samples were characterized using X-ray photoelectron spectroscopy (XPS). The XPS survey spectra confirmed the presence of Bi, Ag and C elements in the Bi/Ag@CC electrode material (Figure 2b). As depicted in Figure 2c, the high-resolution XPS spectra of Bi 4f exhibited distinct peaks at binding energies of 164.5 eV and 159.4 eV, which can be unambiguously assigned to the $4f_{5/2}$ and $4f_{7/2}$ states of Bi⁰, respectively, in accordance with previous reports [31,32]. This observation provided direct evidence for the successful in situ synthesis of bismuth film on CC surfaces. Furthermore, Figure 2d presents the XPS spectra of Ag, revealing fitted peaks at binding energies of 368.1 eV and 374.3 eV, which correspond to the $3d_{5/2}$ and $3d_{3/2}$ states of Ag⁰, respectively.

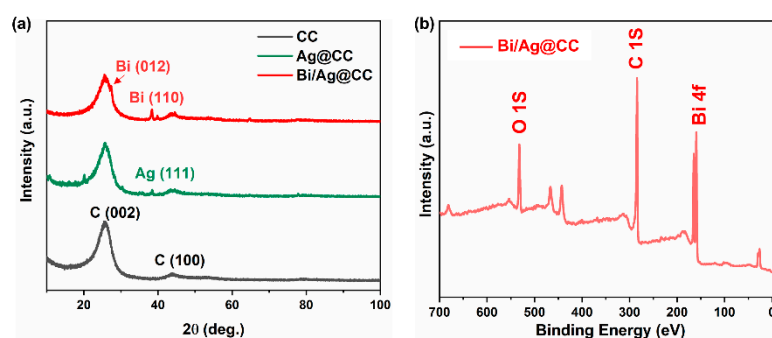


Figure 2. Cont.

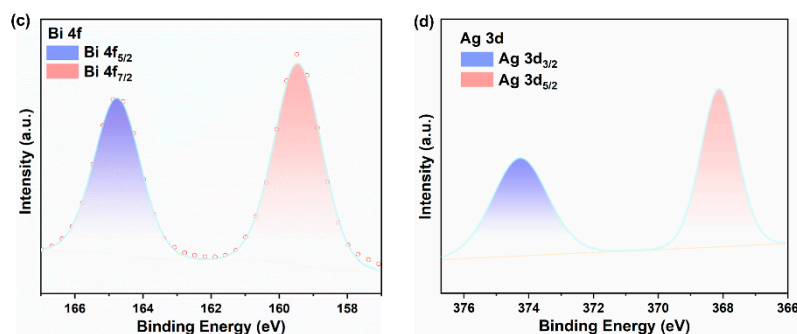


Figure 2. The characteristics of phase structure and elemental composites of Bi/Ag@CC. (a) XRD patterns of different treatment samples. (b–d) The XPS spectra of Bi/Ag@CC.

3.2. Electrochemical Characteristics

The electrochemical properties of the Bi/Ag@CC electrode materials were examined using the $[\text{Fe}(\text{CN})_6]^{3-/-4-}$ redox probe through cyclic voltammetry conducted at a scanning rate of 50 mV/s (Figure 3a). Additionally, Figure 3b illustrates the evolution of the redox peak current in cyclic voltammetry curves as the scanning rate increased in $[\text{Fe}(\text{CN})_6]^{3-/-4-}$ solution. Notably, the anodic current associated with the oxidation of $\text{Fe}^{2+}/\text{Fe}^{3+}$ on the Bi/Ag@CC electrode increased proportionally with the scan rate. Figure 3b shows that the CV curve recorded at 150 mV/s exhibited the highest redox peak current, which demonstrated that as the scanning rate rose, the peak redox current was also augmented. Figure 3c presents the EIS curves of Bi/Ag@CC, Ag@CC and CC, which were measured over a frequency range of 0.01–100 kHz. These curves revealed that the electron-transfer resistance (Rct), a metric reflecting the interfacial properties of the electrode materials, was 5.6 Ω , 6.1 Ω and 46.3 Ω for Bi/Ag@CC, Ag@CC and bare CC, respectively. Based on the measurement results, the findings revealed that the Rct value of Bi/Ag@CC was lower compared to both Ag@CC and CC electrodes, indicating that the Bi/Ag@CC electrode material possessed superior electrochemical properties compared to other electrode materials, and the deposition of bismuth did not produce a significant alteration in the conductivity of the substrate [33].

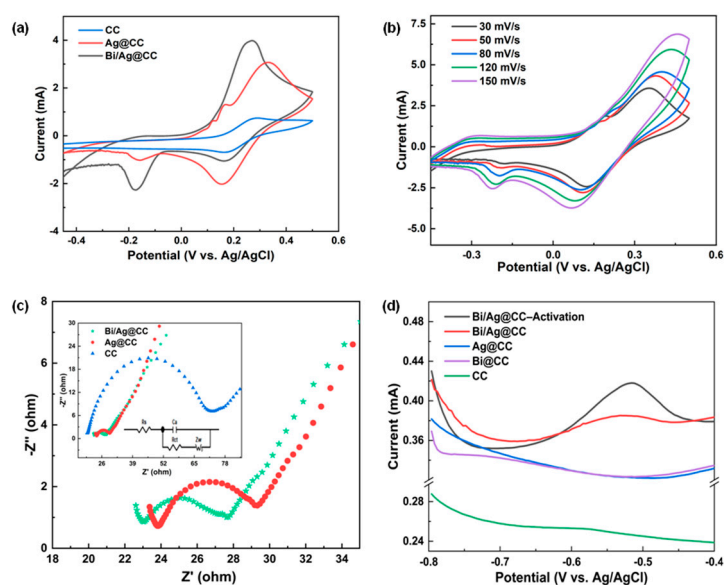


Figure 3. The electrochemical performance of different samples in 5 mmol L⁻¹ $[\text{Fe}(\text{CN})_6]^{3-/-4-}$ (in 1 mol L⁻¹ KCl solution) electrolyte. (a) CV curves of various prepared samples, (b) CV curves of Bi/Ag@CC with different scanning rate, (c) EIS spectra and (d) DPV response of 100 ppb Pb^{2+} in lead nitrate solution.

The electrochemical performances of the prepared samples in a 100 ppb Pb^{2+} solution are depicted through the DPV curves shown in Figure 3d. The Bi/Ag@CC electrode demonstrated a pronounced electrochemical response, manifesting that the preconcentration process enhances the reduction of heavy metal. Moreover, the activated Bi/Ag@CC electrode material treated with enriched lead exhibited a significantly more prominent peak current, with an increase of 8.53%, suggesting that the process necessitates pre-enrichment treatment rather than direct detection [34]. And, the DPV measurements of the Bi@CC electrode material revealed the minimal peak current, suggesting that the pure bismuth film deposited on the carbon cloth did not exhibit a significant interfacial reaction with heavy metal ions. Similarly, the Ag@CC and carbon cloth electrode displayed limited current peaks, illustrating that the Ag nanoparticle and carbon substrate primarily facilitated the electronic path and did not significantly contribute to the electrochemical detection of heavy metal ions.

3.3. Electrochemical Detection of Pb^{2+}

To further elucidate the electrochemical properties of the Bi/Ag@CC electrode materials in detecting heavy metal ions, a comprehensive analysis of critical parameters, including electrolyte pH, deposition voltage and enrichment time, were conducted. Figure 4a displays the current peak response of the Bi/Ag@CC electrode with a pH range of 3.0 to 9.0, with a Pb^{2+} concentration of 100 ppb. The acidity–alkalinity of the electrolyte was adjusted by nitric acid and sodium hydroxide solution. The testing results demonstrated that the peak current of Pb^{2+} on the Bi/Ag@CC electrode increased under acidic conditions. However, as the acidity increased, bubbles were observed on the electrode surface when pH of the electrolyte was 3.0, potentially due to the interference from the hydrogen evolution reaction with the dissolution of Pb^{2+} ions. For weak acid solution, the current signal decreased sharply. In alkaline environment, the sample electrode was damaged, resulting in a reduced peak current. Therefore, the optimized electrolyte pH of 4.5 was chosen for the subsequent experiments. Figure 4b displays the variation in peak currents with respect to various deposition potentials, ranging from -1.3 to -0.8 V. The maximum peak current value was observed at -1.2 V, leading to the selection of -1.2 V as the optimal deposition voltage for depositing Pb^{2+} on the Bi/Ag@CC electrode surface. Furthermore, Figure 4c explores the relationship between the peak current and pre-enrichment time (pH = 3, -1.2 V), with the experimental results illustrating that the current peak is at 360 s. Consequently, 360 s was deemed as the optimal deposition time for the subsequent measurements.

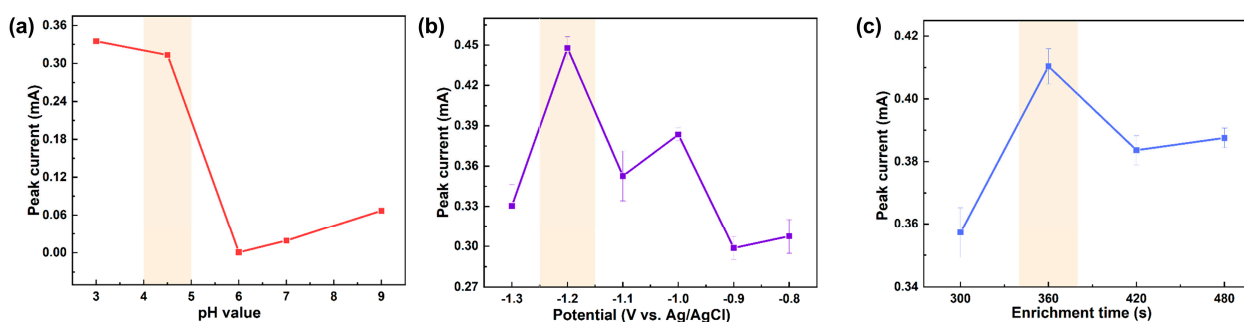


Figure 4. Influence of pH value (a), deposition potential (b) and pre-concentration time (c) on the DPV peak currents of Bi/Ag@CC in 100 ppb Pb^{2+} solution.

During the conventional DPV measurement for heavy metal ion detection, two distinct electrochemical reactions occur on the electrode surface. Firstly, a fixed duration of negative electrodeposition potential was applied to deposit the targeted metallic ions onto the electrode surface. Then, these deposited metallic ions were dissolved by oxidation to metal ions with a specified potential under the DPV measurement mode, resulting in a distinct current peak [35,36]. Figure 5a describes the DPV response of the Bi/Ag@CC

electrochemical detection of Pb^{2+} across a concentration range of 20 ppb to 400 ppb. And, the current variation in lead ion with a concentration of 5 ppb could be observed by the electrochemical sensor, as shown in Figure S4. Figure 5b showcases the peak current values at -0.47 V, demonstrating a linear relationship between the peak current and the Pb^{2+} concentration. The linear equation was calculated as $I_p (\mu\text{A}) = 312.6 \times 0.97C$ (ppb) ($R^2 = 0.995$) for the concentration of Pb^{2+} ranging from 20 to 300 ppb and $I_p (\mu\text{A}) = 542.2 \times 1.89C$ (ppb) ($R^2 = 0.956$) for the concentration of Pb^{2+} ranging from 300 to 400 ppb. Moreover, the limit of detection (LOD) value for Pb^{2+} was evaluated to be 0.15 ppb ($\text{LOD} = 3\sigma/S$). The low LOD may be attributed to the shape of the calibration curve and the variability in the blank signal [37,38]. To investigate the electrochemical detection process between the sample electrodes and heavy metal ions, Figure S5 depicts the elemental mapping of Bi/Ag@CC following DPV measurements, revealing the presence of trace amounts of lead on the surface of the electrode material.

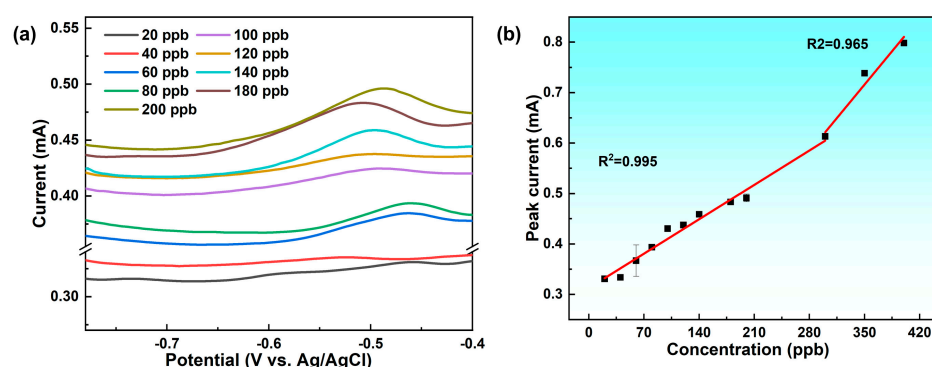


Figure 5. (a) DPV responses at Bi/Ag@CC electrode with various concentrations of Pb^{2+} , and (b) the calibration curves of voltametric curves.

The practical application capabilities of the electrochemical sensor hinge crucially on its selectivity, stability and reproducibility. Considering that the presence of non-target ions in electrolytes may disturb the detection outcome of Bi/Ag@CC, a thorough examination of detection accuracy in the presence of various interfering ions such as Cl^- , SO_4^{2-} , HCO_3^- , Zn^{2+} and CO_3^{2-} was performed. As Figure 6a illustrates, the experimental results exhibit acceptable anti-interference performance for Pb^{2+} detection. Figure 6b showcases the peak current during repeatable testing, which experienced a 2.94% reduction after four measurement cycles. This slight decline could be attributed to the weakening of the bismuth film's performance on the carbon cloth surface due to the enrichment process. Furthermore, to evaluate the repeatability feature, the DPV responses (Pb ions at 100 ppb) of six Bi/Ag@CC samples produced using the same fabrication process are illustrated in Figure 6c. The obtained data demonstrated a relative standard deviation (RSD) of 2.31% for the peak current, manifesting the acceptable reproducibility of Bi/Ag@CC electrode materials. When compared to other reported detection strategies, the sensor presented in this work offers an acceptable linear range and superior detection performance (Table 1). Furthermore, to assess the practical utility of Bi/Ag@CC, tap water and lake water samples were collected and analyzed. These samples were spiked with different concentrations of Pb^{2+} and measured by DPV. The results, presented in Table 2, demonstrate that Bi/Ag@CC, as electrochemical electrode material, exhibited relatively high precision and was capable of detecting Pb^{2+} in actual samples.

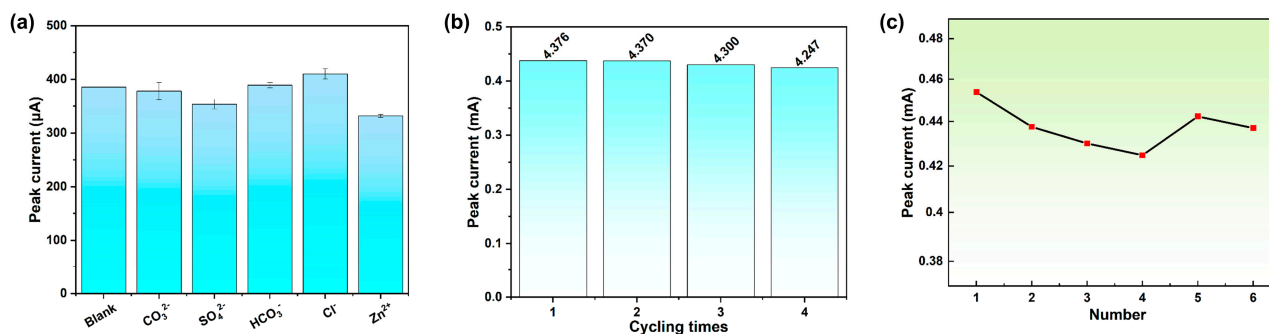


Figure 6. (a) The peak current values of Bi/Ag@CC with 100 ppb Pb²⁺ containing various ions, (b) the peak current values of Bi/Ag@CC with 100 ppb Pb²⁺ for four cycling testing and (c) the reproductivity testing.

Table 1. Comparison of various Bi-based electrodes for determination of Pb²⁺.

Electrode Materials	Technique	Linear Range (ppb)	LOD (ppb)	Ref.
BiCuFE	SWASV	47.5–632.4	1.2	[39]
BiCu _{0.5} -ANPs@CF/SPCE	SWASV	5–150	0.95	[27]
Bi-MWCNTs-CPE	DPASV	41.4–414.4	8.97	[40]
Bi/SPCE	ASV	5–100	0.97	[41]
MXA-CuO/CC	DPASV	4–1200	0.2	[34]
Bi/Uio-66-NH ₂ @CNHs	DPV	200–800	10.56	[7]
Bi/AuNP-SPCE	DPV	1–150	0.03	[42]
Bi/Ag@CC	DPV	20–300	0.15	This work

Table 2. The determination of Pb²⁺ in real samples.

Sample	Spiked (µM)	Found (µM)	Recovery (%)	RSD (% n = 3)
Tap water	80	76.93	96.20	1.81
	100	90.88	90.88	8.7
Lake water	70	68.31	97.60	1.46
	90	79.44	88.26	8.27

4. Conclusions

In summary, this paper presents the development of a bismuth film composite supported by carbon cloth, serving as electrode materials for the electrochemical detection of heavy metal ions. Through the optimization of electrochemical parameters, the optimal deposition potential and preconcentration time for DPV measurements were identified as -1.2 V and 360 s, respectively. Furthermore, the impact of varying targeted ion concentrations (5–400 ppb) and pH values (3–9) on the detection performance was examined. The resulting sensor demonstrated an impressive linear range of 20–300 ppb, with detection limits reaching 0.15 ppb for Pb²⁺ ions. Notably, it exhibited excellent anti-interference capabilities and satisfactory repeatability, with an RSD of less than 2.31% ($n = 6$). Additionally, the simplicity of the in situ electrodeposition synthesis strategy, cost-effective non-precious reactants and remarkable detection performance collectively position this bismuth-based composite as a promising candidate for practical electrochemical sensing applications.

Supplementary Materials: The following supporting information can be downloaded at: <https://www.mdpi.com/article/10.3390/chemosensors12060103/s1>, Figure S1: The resistance variation in Ag@CC with the soaking time. Figure S2: The electrodeposition parameters of bismuth film. (a) Deposition potential and (b) deposition time for the Bi film on the Ag@CC surface. Figure S3: XRD spectra of Bi@CC. Figure S4: The current variation in the electrochemical sensor for lead ions in concentration of 5 ppb. Figure S5: SEM images and elemental mapping of Bi/Ag@CC following DPV testing.

Author Contributions: Conceptualization, Y.Z. (Yang Zhao) and J.-H.F.; methodology, Y.C., Y.Z. (Yang Zhao) and J.X.; validation, Y.C., Y.Z. (Yun Zeng), M.Y. and Z.W.; formal analysis, Y.L., J.X. and M.Y.; investigation, Y.C., X.Z. and Z.W.; resources, Y.Z. (Yun Zeng) and J.X.; data curation, Y.L., X.Z., Y.Z. (Yun Zeng) and Y.C.; writing—original draft preparation, Y.C. and J.-H.F.; writing—review and editing, Y.Z. (Yun Zeng), Y.Z. (Yang Zhao) and J.-H.F.; funding acquisition, Y.Z. (Yang Zhao). All authors have read and agreed to the published version of the manuscript.

Funding: This work was supported by the Natural Science Foundation of Sichuan Province (Grant No. 2023NSFSC1068), and the authors thank the Open Fund Project of Hubei Key Laboratory of Mine Environmental Pollution Control and Remediation (2023XZ106).

Institutional Review Board Statement: Not applicable.

Informed Consent Statement: Not applicable.

Data Availability Statement: Data are contained within the article.

Conflicts of Interest: The authors declare no conflicts of interest.

References

1. Zamora-Ledezma, C.; Negrete-Bolagay, D.; Figueroa, F.; Zamora-Ledezma, E.; Ni, M.; Alexis, F.; Guerrero, V.H. Heavy metal water pollution: A fresh look about hazards, novel and conventional remediation methods. *Environ. Technol. Innov.* **2021**, *22*, 101504. [[CrossRef](#)]
2. Gonzalez, K.A.; Kazemeini, S.; Weber, D.C.; Cordero, P.A.; Garcia, E.M.; Rusinek, C.A. Electrochemical sensing of heavy metals in biological media: A review. *Electroanalysis* **2023**, *35*, e202300098. [[CrossRef](#)]
3. Li, B.; Xie, X.; Meng, T.; Guo, X.; Li, Q.; Yang, Y.; Jin, H.; Jin, C.; Meng, X.; Pang, H. Recent advance of nanomaterials modified electrochemical sensors in the detection of heavy metal ions in food and water. *Food Chem.* **2024**, *440*, 138213. [[CrossRef](#)]
4. Mohanadas, D.; Rohani, R.; Sulaiman, Y.; Bakar, S.A.; Mahmoudi, E.; Zhang, L.-C. Heavy metal detection in water using MXene and its composites: A review. *Mater. Today Sustain.* **2023**, *22*, 100411. [[CrossRef](#)]
5. Li, H.; Zhao, J.; Zhao, S.; Cui, G. Simultaneous determination of trace Pb(II), Cd(II), and Zn(II) using an integrated three-electrode modified with bismuth film. *Microchem. J.* **2021**, *168*, 106390. [[CrossRef](#)]
6. Gao, J.; He, D.; Zhang, J.; Sun, B.; Wang, G.; Suo, H.; Zhang, L.; Zhao, C. In-situ growth of porous rod-like tungsten oxide for electrochemical determination of cupric ion. *Anal. Chim. Acta* **2023**, *1276*, 341645. [[CrossRef](#)] [[PubMed](#)]
7. Chu, J.; Chu, B.; Lu, C.; Gu, Q.; Li, W.; Lin, R.; Lu, J.; Chen, X. Highly sensitive detection of lead ions and cadmium ions based on UiO-66-NH₂@carbon nanohorns composites enhanced by bismuth film in water environment. *J. Environ. Chem. Eng.* **2022**, *10*, 108753. [[CrossRef](#)]
8. Ansari, A.A.; Khan, A.M.; Salem, M.A.S.; Bhat, A.S. Synthesis and characterization of Ni@UiO-66 Metal-Organic Framework for fluorescence detection of heavy metal ions in the aqueous phase. *Mater. Chem. Phys.* **2024**, *318*, 129245. [[CrossRef](#)]
9. Tian, C.; Lee, Y.; Song, Y.; Elmasry, M.R.; Yoon, M.; Kim, D.-H.; Cho, S.-Y. Machine-learning enhanced fluorescent nanosensor based on carbon quantum dots for heavy metal detection. *ACS Appl. Nano Mater.* **2024**, *7*, 5576–5586.
10. Chen, Z.; Zhang, Z.; Qi, J.; You, J.; Ma, J.; Chen, L. Colorimetric detection of heavy metal ions with various chromogenic materials: Strategies and applications. *J. Hazard. Mater.* **2023**, *441*, 129889. [[CrossRef](#)]
11. Nataraj, N.; Dash, P.; Sakthivel, R.; Lin, Y.-C.; Fang, H.-W.; Chung, R.-J. Simultaneous electrochemical and colorimetric detection of tri-heavy metal ions in environmental water samples employing 3D-MOF/nickel selenide as a synergistic catalyst. *Chem. Eng. J.* **2024**, *485*, 149965. [[CrossRef](#)]
12. Li, L.; Bi, X.; Zhen, M.; Ren, Y.; Zhang, L.; You, T. Recent advances in analytical sensing detection of heavy metal ions based on covalent organic frameworks nanocomposites. *Trends Anal. Chem.* **2024**, *171*, 117488. [[CrossRef](#)]
13. Manikandan, R.; Yoon, J.-H.; Chang, S.-C. Emerging Trends in nanostructured materials-coated screen printed electrodes for the electrochemical detection of hazardous heavy metals in environmental matrices. *Chemosphere* **2023**, *344*, 140231. [[CrossRef](#)] [[PubMed](#)]
14. Tang, X.; Zhang, Q.Q.; Chen, D.Y.; Deng, L.F.; He, Y.X.; Wang, J.X.; Pan, C.Y.; Tang, J.T.; Yu, G.P. Thiol-grafted covalent organic framework-based electrochemical platforms for sensitive detection of Hg(II) ions. *Chem. Commun.* **2023**, *59*, 8731–8734. [[CrossRef](#)] [[PubMed](#)]
15. Winiarski, J.P.; Melo, D.J.D.; Santana, E.R.; Santos, C.S.; de Jesus, C.G.; Fujiwara, S.T.; Wohnrath, K.; Pessoa, C.A. Layer-by-layer films of silsesquioxane and nickel (II) tetrasulphophthalocyanine as glucose oxidase platform immobilization: Amperometric determination of glucose in kombucha beverages. *Chemosensors* **2023**, *11*, 346. [[CrossRef](#)]
16. Zamarchi, F.; Silva, T.R.; Winiarski, J.P.; Santana, E.R.; Vieira, I.C. Polyethylenimine-based electrochemical sensor for the determination of caffeic acid in aromatic herbs. *Chemosensors* **2022**, *10*, 357. [[CrossRef](#)]

17. Bressi, V.; Celesti, C.; Ferlazzo, A.; Len, T.; Moulae, K.; Neri, G.; Luque, R.; Espro, C. Waste-derived carbon nanodots for fluorimetric and simultaneous electrochemical detection of heavy metals in water. *Environ. Sci. Nano* **2024**, *11*, 1245–1258. [[CrossRef](#)]
18. Sun, Z.; Wang, Y.; Liu, T.; Kong, X.; Pan, T.; Zhang, F.; Lei, X.; Duan, X. Super-stable mineralization of Cu, Cd, Zn and Pb by CaAl-layered double hydroxide: Performance, mechanism, and large-scale application in agriculture soil remediation. *J. Hazard. Mater.* **2023**, *447*, 130723. [[CrossRef](#)]
19. Shafqat, S.S.; Rizwan, M.; Batool, M.; Shafqat, S.R.; Mustafa, G.; Rasheed, T.; Zafar, M.N. Metal organic frameworks as promising sensing tools for electrochemical detection of persistent heavy metal ions from water matrices: A concise review. *Chemosphere* **2023**, *318*, 137920. [[CrossRef](#)] [[PubMed](#)]
20. Hu, H.; Yan, M.; Jiang, J.; Huang, A.; Cai, S.; Lan, L.; Ye, K.; Chen, D.; Tang, K.; Zuo, Q.; et al. A state-of-the-art review on biomass-derived carbon materials for supercapacitor applications: From precursor selection to design optimization. *Sci. Total Environ.* **2024**, *912*, 169141. [[CrossRef](#)]
21. Wang, C.; Du, L.; Xing, X.; Feng, D.; Tian, Y.; Li, Z.; Yang, D. Flexible carbon cloth in-situ assembling WO₃ microsheets bunches with Ni dopants for non-enzymatic glucose sensing. *Appl. Surf. Sci.* **2022**, *586*, 152822. [[CrossRef](#)]
22. Shao, P.; Chang, Z.; Li, M.; Lu, X.; Jiang, W.; Zhang, K.; Luo, X.; Yang, L. Mixed-valence molybdenum oxide as a recyclable sorbent for silver removal and recovery from wastewater. *Nat. Commun.* **2023**, *14*, 1365. [[CrossRef](#)] [[PubMed](#)]
23. Jiang, Y.; Cui, S.; Xia, T.; Sun, T.; Tan, H.; Yu, F.; Su, Y.; Wu, S.; Wang, D.; Zhu, N. Real-time monitoring of heavy metals in healthcare via twistable and washable smartsensors. *Anal. Chem.* **2020**, *92*, 14536–14541. [[CrossRef](#)] [[PubMed](#)]
24. Feng, Y.; Zhao, H.; Feng, T.; Liu, X.; Lan, M. Conductive nitrogen-doped carbon nanosheet-encapsulates bismuth nanoparticles for simultaneous high-performance detection of Cd(II) and Pb(II). *Microchem. J.* **2024**, *197*, 109881. [[CrossRef](#)]
25. Wang, C.; Niu, Q.; Liu, D.; Dong, X.; You, T. Electrochemical sensor based on Bi/Bi₂O₃ doped porous carbon composite derived from Bi-MOFs for Pb²⁺ sensitive detection. *Talanta* **2023**, *258*, 124281. [[CrossRef](#)] [[PubMed](#)]
26. De Penning, R.; Padalkar, S. Detection of lead and cadmium with electrochemically reduced grapheme oxide-carbon cloth sensors. *MRS Commun.* **2023**, *13*, 1427–1432. [[CrossRef](#)]
27. Huang, A.; Guo, Y.; Zhu, Y.; Chen, T.; Yang, Z.; Song, Y.; Wasnik, P.; Li, H.; Peng, S.; Guo, Z.; et al. Durable washable wearable antibacterial thermoplastic polyurethane/carbon nanotube@silver nanoparticles electrospun membrane strain sensors by multi-conductive network. *Adv. Compos. Hybrid Mater.* **2023**, *6*, 101. [[CrossRef](#)]
28. Zhang, W.; Guo, T.; Liu, Y.; Zhang, X.; Zou, B.; Zhao, C.; Suo, H.; Wang, H.; Zhao, X. Electrocatalytic performance of carbon layer and spherical carbon/carbon cloth composites towards hydrogen evolution from the direct electrolysis of bunsen reaction product. *Chem. Res. Chin. Univ.* **2023**, *40*, 109–118. [[CrossRef](#)]
29. Shi, H.; Zhang, C.; Zhan, J.; Chen, J.; Li, X.; Gao, Z.; Li, Z. Bi Nanosheets on porous carbon cloth composites for ultrastable flexible nickel–bismuth batteries. *ACS Appl. Mater. Interfaces* **2023**, *15*, 36190–36200. [[CrossRef](#)]
30. Hu, M.; He, H.; Xiao, F.; Liu, C. Bi-MOF-derived carbon wrapped Bi nanoparticles assembly on flexible graphene paper electrode for electrochemical sensing of multiple heavy metal ions. *Nanomater* **2023**, *13*, 2069. [[CrossRef](#)]
31. He, Y.; Wang, Z.; Ma, L.; Zhou, L.; Jiang, Y.; Gao, J. Synthesis of bismuth nanoparticle-loaded cobalt ferrite for electrochemical detection of heavy metal ions. *RSC Adv.* **2020**, *10*, 27697–27705. [[CrossRef](#)] [[PubMed](#)]
32. Zeng, Y.; Wang, M.; He, W.; Fang, P.; Wu, M.; Tong, Y.; Chen, M.; Lu, X. Engineering high reversibility and fast kinetics of Bi nanoflakes by surface modulation for ultrastable nickel–bismuth batteries. *Chem. Sci.* **2019**, *10*, 3602–3607. [[CrossRef](#)] [[PubMed](#)]
33. Yin, H.; He, H.; Li, T.; Hu, M.; Huang, W.; Wang, Z.; Yang, X.; Yao, W.; Xiao, F.; Wu, Y.; et al. Ultra-sensitive detection of multiplexed heavy metal ions by MOF-derived carbon film encapsulating BiCu alloy nanoparticles in potable electrochemical sensing system. *Anal. Chim. Acta* **2023**, *1239*, 340730. [[CrossRef](#)] [[PubMed](#)]
34. Gao, J.; Yin, J.; Wang, G.; Wang, X.; Zhang, J.; Sun, B.; He, D.; Suo, H.; Zhao, C. A novel electrode for simultaneous detection of multiple heavy metal ions without pre-enrichment in food samples. *Food Chem.* **2024**, *448*, 138994. [[CrossRef](#)] [[PubMed](#)]
35. Wen, L.; Dong, J.; Yang, H.; Zhao, J.; Hu, Z.; Han, H.; Hou, C.; Luo, X.; Huo, D. A novel electrochemical sensor for simultaneous detection of Cd²⁺ and Pb²⁺ by MXene aerogel-CuO/carbon cloth flexible electrode based on oxygen vacancy and bismuth film. *Sci. Total Environ.* **2022**, *851*, 158325. [[CrossRef](#)]
36. Jeong, S.; Yang, S.; Lee, Y.J.; Lee, S.H. Laser-induced graphene incorporated with silver nanoparticles applied for heavy metal multi-detection. *J. Mater. Chem. A* **2023**, *11*, 13409–13418. [[CrossRef](#)]
37. Kim, M.; Park, J.; Park, H.; Jo, W.; Lee, W.; Park, J. Detection of heavy metals in water environment using nafion-blanketed bismuth nanoplates. *ACS Sustain. Chem. Eng.* **2023**, *11*, 6844–6855. [[CrossRef](#)]
38. Bayram, L.; Guler, M. An ultra-sensitive non-enzymatic hydrogen peroxide sensor based on SiO₂-APTES supported Au nanoparticles modified glassy carbon electrode. *Prog. Nat. Sci. Mater. Int.* **2019**, *29*, 390–396. [[CrossRef](#)]
39. Finšgar, M.; Kovačec, L. Copper-bismuth-film in situ electrodes for heavy metal detection. *Microchem. J.* **2020**, *154*, 104635. [[CrossRef](#)]
40. de Borba, W.G.; Guedes, K.C.F.; da Silva, J.G. Construction of a carbon paste electrode modified with multi-walled carbon nanotubes and bismuth for voltammetric simultaneous determination of Cd²⁺ and Pb²⁺. *Rev. Virtual Quím.* **2021**, *13*, 1042–1050. [[CrossRef](#)]

41. Ninwong, B.; Ratnarathorn, N.; Henry, C.S.; Mace, C.R.; Dungchai, W. Dual Sample preconcentration for simultaneous quantification of metal ions using electrochemical and colorimetric assays. *ACS Sens.* **2020**, *5*, 3999–4008. [[CrossRef](#)] [[PubMed](#)]
42. Lu, Z.; Zhang, J.; Dai, W.; Lin, X.; Ye, J.; Ye, J. A screen-printed carbon electrode modified with a bismuth film and gold nanoparticles for simultaneous stripping voltammetric determination of Zn(II), Pb(II) and Cu(II). *Microchim. Acta* **2017**, *184*, 4731–4740. [[CrossRef](#)]

Disclaimer/Publisher’s Note: The statements, opinions and data contained in all publications are solely those of the individual author(s) and contributor(s) and not of MDPI and/or the editor(s). MDPI and/or the editor(s) disclaim responsibility for any injury to people or property resulting from any ideas, methods, instructions or products referred to in the content.